Histone hypercitrullination mediates chromatin decondensation and neutrophil extracellular trap formation

Yanming Wang,[1] Ming Li,[1] Sonja Stadler,[2,3] Sarah Correll,[4] Pingxin Li,[1] Danchen Wang,[1] Ryo Hayama,[2] Lauriebeth Leonelli,[2] Hyunsil Han,[5,6] Sergei A. Grigoryev,[4] C. David Allis,[3] and Scott A. Coonrod[2]

[1]Center for Gene Regulation, Department of Biochemistry and Molecular Biology, Pennsylvania State University, University Park, PA 16802
[2]Baker Institute for Animal Health, College of Veterinary Medicine, Cornell University, Ithaca, NY 14853
[3]Laboratory of Chromatin Biology, The Rockefeller University, New York, NY 10065
[4]Department of Biochemistry and Molecular Biology, Pennsylvania State University College of Medicine, Hershey, PA 17033
[5]Department of Microbiology and [6]Department of Immunology, Weill Medical College of Cornell University, New York, NY 10021

Peripheral blood neutrophils form highly decondensed chromatin structures, termed neutrophil extracellular traps (NETs), that have been implicated in innate immune response to bacterial infection. Neutrophils express high levels of peptidylarginine deiminase 4 (PAD4), which catalyzes histone citrullination. However, whether PAD4 or histone citrullination plays a role in chromatin structure in neutrophils is unclear. In this study, we show that the hypercitrullination of histones by PAD4 mediates chromatin decondensation. Histone hypercitrullination is detected on highly decondensed chromatin in HL-60 granulocytes and blood neutrophils. The inhibition of PAD4 decreases histone hypercitrullination and the formation of NET-like structures, whereas PAD4 treatment of HL-60 cells facilitates these processes. The loss of heterochromatin and multilobular nuclear structures is detected in HL-60 granulocytes after PAD4 activation. Importantly, citrullination of biochemically defined avian nucleosome arrays inhibits their compaction by the linker histone H5 to form higher order chromatin structures. Together, these results suggest that histone hypercitrullination has important functions in chromatin decondensation in granulocytes/neutrophils.

Introduction

In eukaryotic cells, 147 bp of DNA is tightly packed around a core histone octamer (including two of each of the histones H3, H2B, H2A, and H4) to form a nucleosome core particle (Kornberg and Lorch, 1999; Richmond and Davey, 2003). The formation of higher order chromatin structures is further mediated by linker DNA and linker histones (Schalch et al., 2005; Brown and Schuck, 2006; Fan and Roberts, 2006; Kan et al., 2007). In particular, the binding of linker histones to the 11-nm polynucleosomal fiber plays an important role in chromatin compaction to form a 30-nm fiber. However, the dynamic regulation of chromatin higher order structures during transcription and other nuclear events remains largely unclear.

Posttranslational modification of histone proteins such as acetylation, phosphorylation, and methylation regulates various chromatin functions, including transcription, DNA damage repair, and chromatin condensation/decondensation (Shilatifard, 2006; Kouzarides, 2007; Li et al., 2007). To explain the biological significance of histone modifications in chromatin biology, a "histone code" hypothesis has been proposed, which predicts that covalent histone modifications working singularly or in combination regulate histone structure and multiple nuclear functions (Strahl and Allis, 2000; Turner, 2000; Jenuwein and Allis, 2001).

Peptidylarginine deiminases (PADs) are a family of enzymes previously known to convert protein arginine (Arg) to citrulline (Cit), a nonconventional amino acid in proteins (Vossenaar et al., 2003). PAD4 (also called PADI4/PADV) was first identified in human HL-60 leukemia cells upon differentiation

Correspondence to Yanming Wang: yuw12@psu.edu; or Scott A. Coonrod: sac269@cornell.edu

Abbreviations used in this paper: Cit, citrulline; MNase, micrococcal nuclease; NET, neutrophil extracellular trap; PAD, peptidylarginine deiminase.

The Rockefeller University Press $30.00
J. Cell Biol. Vol. 184 No. 2 205–213
www.jcb.org/cgi/doi/10.1083/jcb.200806072

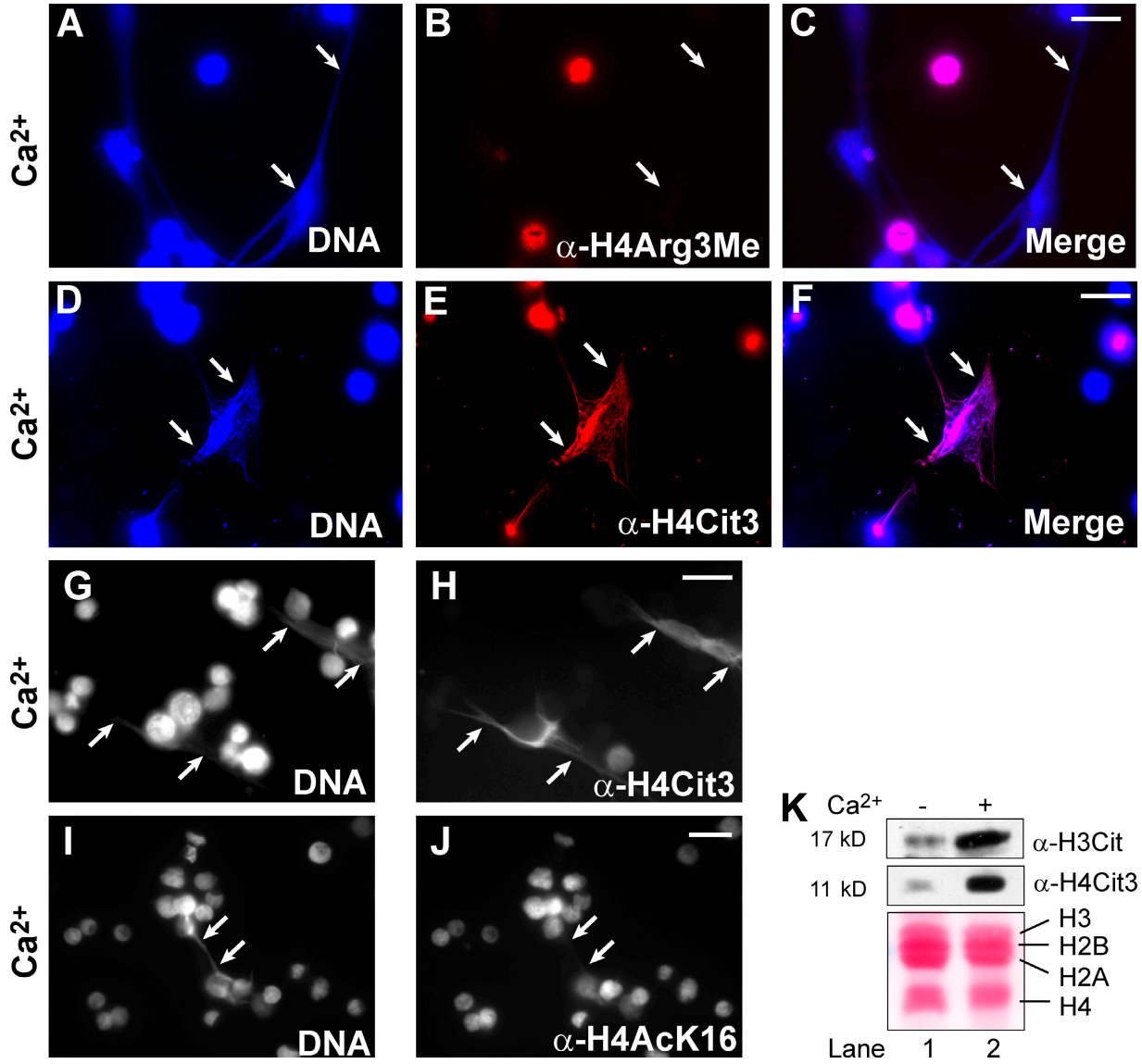

Figure 1. **Chromatin decondensation induced by PAD4 activation and histone citrullination in HL-60 granulocytes.** (A–C) Loss of histone H4Arg3 methylation on the decondensed chromatin (denoted by arrows) after calcium ionophore treatment. (D–F) Increase in H4Cit3 on the decondensed chromatin (denoted by arrows). (G and H) Grayscale images show an increase of H4Cit3 on decondensed chromatin (denoted by arrows). (I and J) Grayscale images show that H4K16 acetylation was not elevated on the decondensed chromatin (denoted by arrows). (K) Changes in histone H3 and H4 citrullination analyzed by Western blotting. Ponceau S staining shows the amount of histones. Bars, 20 µm.

along the granulocyte lineage (Nakashima et al., 1999) and is highly expressed in peripheral blood neutrophils (Nakashima et al., 2002; Su et al., 2004). PAD4 mainly localizes to the nucleus and targets histones H3, H2A, and H4 for citrullination (Hagiwara et al., 2002; Nakashima et al., 2002; Cuthbert et al., 2004; Wang et al., 2004). We have previously shown that PAD4 also converts histone methylarginine residues to Cit by a novel reaction termed demethylimination, and this activity of PAD4 counteracts the functions of histone Arg methylation at estrogen target genes (Wang et al., 2004). Recently, we have reported that PAD4 functions as a corepressor of p53 to regulate histone Arg modification and gene expression (Li et al., 2008; Yao et al., 2008). These studies support a view that promoter-specific histone citrullination is involved in gene regulation.

In response to various stimuli, including pathogen infection and inflammatory response, neutrophils form a highly decondensed chromatin structure, termed neutrophil extracellular traps (NETs), as an innate immune response (Brinkmann et al., 2004; Beiter et al., 2006; Buchanan et al., 2006; Fuchs et al., 2007). However, whether any histone modification plays a role during this change of chromatin higher order structure is largely unknown. In this study, we show that in addition to its gene regulatory role, PAD4-catalyzed histone hypercitrullination appears to play a critical role in chromatin decondensation in granulocytes/neutrophils. Our results support a model in which global histone hypercitrullination regulates the unfolding of chromatin structures during NET formation.

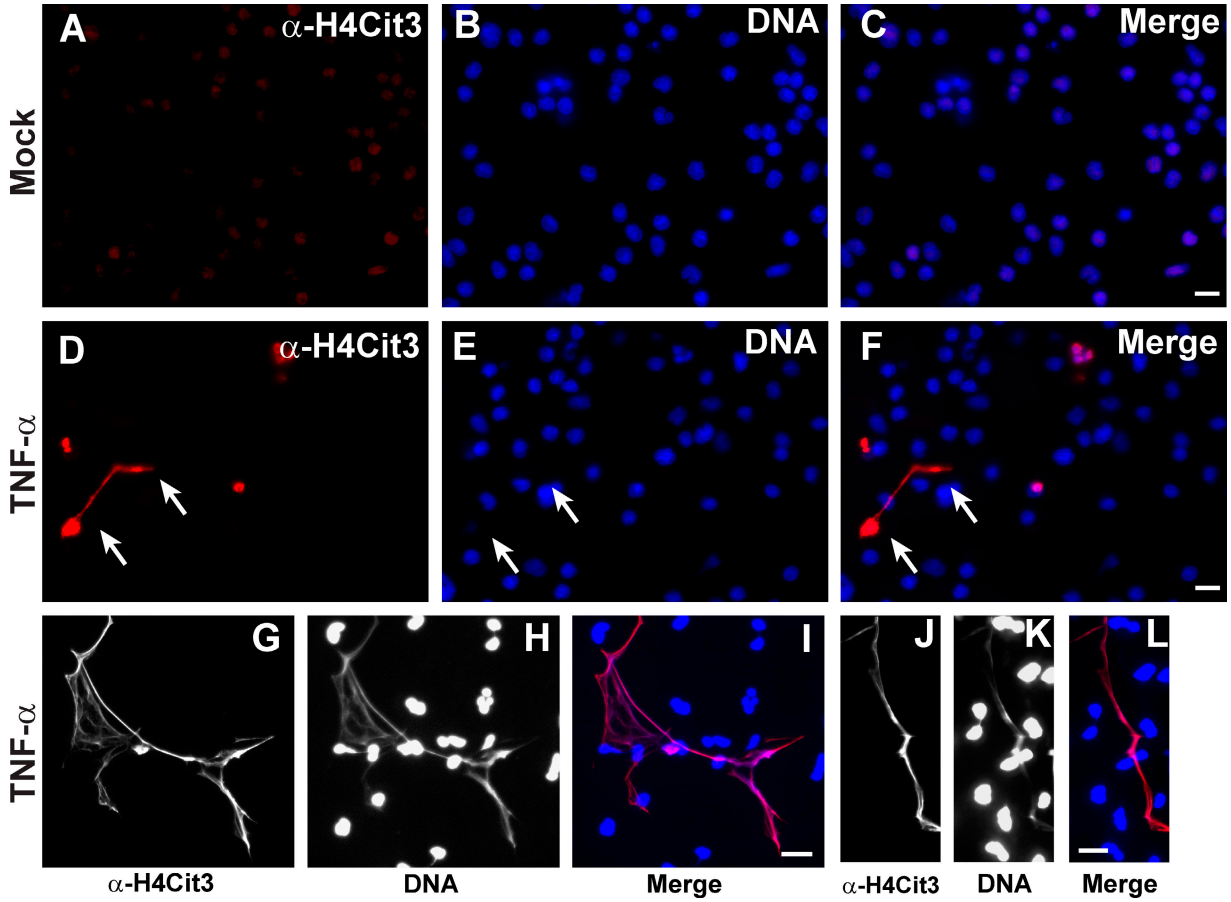

Figure 2. **Histone citrullination on highly decondensed chromatin in peripheral blood neutrophils treated with TNF-α.** (A–C) H4Cit3 staining before TNF-α treatment. (D–F) Approximately 10% of cells were stained with H4Cit3 after 15-min TNF-α treatment. The white arrows denote decondensed chromatin. (G–L) Representative images of NETs stained by both DNA dye and H4Cit3 antibody. Bars, 20 μm.

Results and discussion

Histone hypercitrullination and chromatin decondensation in HL-60 granulocytes

In response to DMSO treatment, HL-60 cells differentiate along the granulocyte lineage and express higher levels of PAD4. Previously, we reported that histone H3Arg2, -8, and -17 residues were citrullinated at 0, 27.3, and 6.5% in HL-60 granulocytes after calcium ionophore treatment (Wang et al., 2004). However, the role of histone hypercitrullination remains unclear. In this study, we found that within 15 min after calcium ionophore treatment, a subset of HL-60–derived granulocytes appear to rupture and release long stretches of extensively decondensed chromatin into the extracellular space, forming weblike chromatin structures (Fig. 1 and Fig. S1, A–C, available at http://www.jcb.org/cgi/content/full/jcb.200806072/DC1). In accordance with our previous finding that PAD4 targets histone methylarginine residues for citrullination (Wang et al., 2004), histone H4Arg3 methylation was decreased (Fig. 1 B) and histone H4Cit3 was increased (Fig. 1, E and H) at regions of highly decondensed chromatin, suggesting that chromatin decondensation is associated with PAD activation. The acetylation of histone H4K16 has been correlated with chromatin decondensation (Robinson et al., 2008). In contrast to H4Cit3, this modification was not increased at the decondensed chromatin fibers (Fig. 1, I and J), suggesting that the increased staining of histone citrullination is unlikely to be the result of an increase in antibody accessibility. To further test the increase in histone citrullination, Western blot experiments were performed. After calcium ionophore treatment, both H4Cit3 and histone H3 citrullination (the α-H3Cit antibody is generated against a Cit2-, Cit8-, and Cit17-containing H3 peptide) were significantly increased (Fig. 1 K).

Induction of hypercitrullination and global chromatin decondensation by TNF-α in peripheral blood neutrophils

Blood neutrophils are known to form highly decondensed chromatin structures, termed NETs, after bacterial infection (Brinkmann et al., 2004; Fuchs et al., 2007). To analyze whether histone hypercitrullination and chromatin decondensation occur in blood neutrophils, we treated neutrophils with the proinflammatory cytokine TNF-α. Before TNF-α treatment, very low levels of H4Cit3 antibody staining were observed in neutrophils (Fig. 2, A–C). After TNF-α treatment for 15 min, ∼10% of neutrophils (>300 cells counted from three independent experiments) showed a dramatic increase in histone citrullination (Fig. 2, D–F), suggesting that PAD4 is activated after TNF-α treatment in a subset of blood neutrophils. A close examination

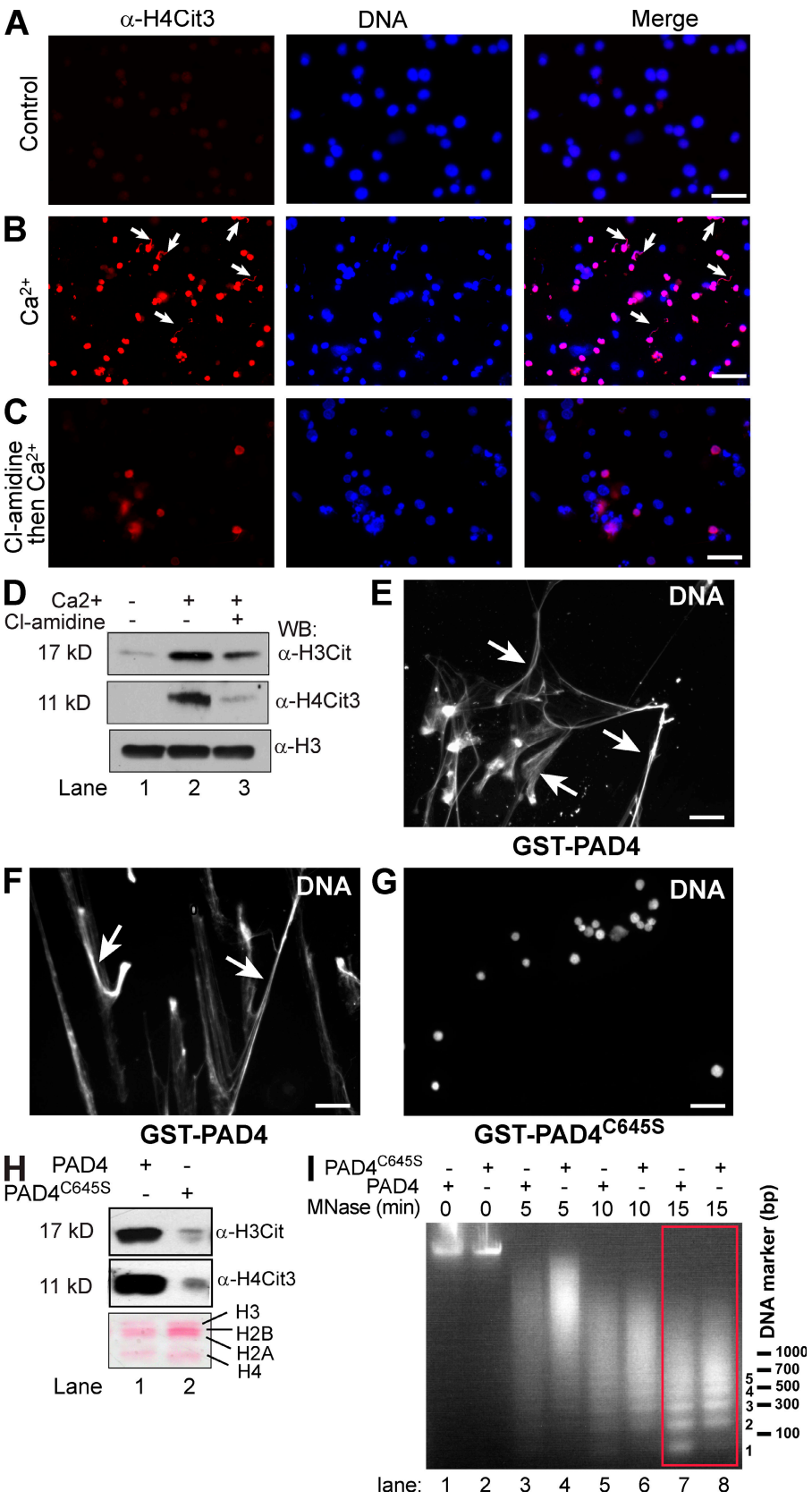

Figure 3. **PAD4 activity is important for the formation of highly decondensed chromatin.** (A–C) H4Cit3 and DNA staining of HL-60 granulocytes without treatment (A), with calcium ionophore treatment (B), and with the PAD4 inhibitor Cl-amidine treatment before calcium ionophore treatment (C). The arrows denote decondensed chromatin stained by the H4Cit3 antibody. (D) Western blot assays of histone H3 and H4 citrullination. The histone H3 blot is a loading control. (E–G) Decondensed chromatin (denoted by arrows) was detected in HL-60 cells after Triton X-100 and GST-PAD4 treatment (E and F) but not after the GST-PAD4^{C645S} mutant treatment (G). (H) Western blot assays of histone H3 and H4 citrullination in HL-60 cells after incubation with GST-PAD4 or the GST-PAD4^{C645S} mutant. Ponceau S staining shows the amount of histones. (I) MNase digestion of HL-60 cells treated with GST-PAD4 or the GST-PAD4^{C645S} mutant. Chromatin in GST-PAD4–treated cells (lane 7) is more accessible than that in GST-PAD4^{C645S}–treated cells (lane 8). The red box highlights lanes with a clear difference in MNase digestion. Bars, 30 µm.

of the decondensed chromatin with NET morphology found that high levels of histone citrullination are associated with decondensed chromatin (Fig. 2, G–L). While we were preparing this manuscript, a study showed that various cytokines and extracellular signals such as TNF, lipopolysaccharide, and H_2O_2 induced histone citrullination and chromatin decondensation in

neutrophils (Neeli et al., 2008). Collectively, these experiments relate histone hypercitrullination to chromatin decondensation during NET formation.

PAD4 activity is important for mediating chromatin decondensation and NET-like chromatin structure formation

To test whether PAD4 activity is important for chromatin decondensation, we treated HL-60 granulocytes with Cl-amidine, a newly synthesized PAD4 inhibitor (Luo et al., 2006), before calcium ionophore treatment. Double staining of HL-60 granulocytes with the H4Cit3 antibody and the DNA dye Hoechst was performed to analyze histone citrullination and the formation of NET-like chromatin structure. Without calcium ionophore treatment, each cell had only weak H4Cit3 staining and did not display NET-like chromatin structure (Fig. 3 A). After calcium ionophore treatment, ∼36% of cells were strongly stained with the H4Cit3 antibody (Fig. 3 B). Notably, >8% of cells formed NET-like chromatin structures (Fig. 3 B, arrows). In contrast, Cl-amidine treatment for 15 min before calcium ionophore treatment decreased the number of cells showing positive H4Cit3 staining (Fig. 3 C). Moreover, NET-like chromatin structure was not observed in cells treated with Cl-amidine before calcium ionophore treatment (Fig. 3 C). The effect of PAD4 inhibition by Cl-amidine on histone H3 and H4 citrullination after calcium ionophore treatment was validated by Western blotting (Fig. 3 D, compare lane 2 with lane 3). These results indicate that PAD activity is important for histone citrullination and chromatin decondensation in HL-60 granulocytes after calcium ionophore treatment.

To test whether PAD4 activity directly induces chromatin decondensation, we analyzed chromatin decondensation in undifferentiated HL-60 cells expressing a low level of endogenous PAD4 (Fig. S1 D). First, HL-60 cells were permeabilized by 0.1% Triton X-100 in PBS solution before treatment with wild-type GST-PAD4 fusion protein or a catalytically inactive GST-PAD4^{C645S} mutant in the PAD assay buffer containing a physiological concentration of NaCl. The addition of the wild-type PAD4 but not the inactive PAD4^{C645S} mutant reproducibly caused pronounced chromatin decondensation (Fig. 3, compare E and F with G). Furthermore, Western blot analyses showed a dramatic increase of histone H3 and H4 citrullination in PAD4-treated cells but not in cells treated with the PAD4^{C645S} mutant (Fig. 3 H). Collectively, we conclude that histone citrullination mediates extensive chromatin decondensation in HL-60 cells permeabilized with Triton X-100.

Micrococcal nuclease (MNase) digests chromatin at the linker DNA region, leading to the release of solubilized poly- and mononucleosome-sized fragments, which is often used as an indication of the accessibility of linker DNA as well as chromatin compaction. The effects of PAD4 treatment on chromatin decondensation prompted us to test whether PAD4 treatment of HL-60 cells alters the accessibility of linker DNA to MNase. After treatment of HL-60 cells with PAD4 or the PAD4^{C645S} mutant, MNase was added to digest chromatin for the time points indicated (Fig. 3 I). MNase digestion generated mononucleosomes more rapidly in cells treated with PAD4 compared with cells treated with the PAD4^{C645S} mutant (Fig. 3 I, compare lane 7 with lane 8). These results indicate that linker DNA is more accessible to MNase after PAD4 treatment. Furthermore, because the size of the nucleosome repeat was not changed as a result of the PAD4 treatment, it appears that the primary nucleosomal structure is not affected by histone citrullination.

PAD4 activity is required for bacteria-mediated chromatin decondensation

To analyze whether PAD4 activity is important for NET formation under more physiologically relevant conditions, we treated HL-60 cells, DMSO-differentiated HL-60 cells, or DMSO-differentiated HL-60 cells pretreated with Cl-amidine with IL-8 and bacteria *Shigella flexneri*, which was shown to induce NET formation in peripheral blood neutrophils (Brinkmann et al., 2004). Histone H3 citrullination was rarely detected in undifferentiated HL-60 cells treated with IL-8 and bacteria *S. flexneri* for 3 h (Fig. 4, A and D). Cells occasionally observed with positive staining may reflect HL-60 cell spontaneous differentiation and PAD4 expression (Fig. S1 D). In contrast, after differentiation along the granulocytic lineage to increase PAD4 expression (Fig. S1 D) and IL-8 and bacteria treatment, 9.8 ± 0.7% (n = 4) of cells became histone H3 citrullination positive with a concomitant increase of NET formation in 3.2 ± 0.1% (n = 4) of cells (Fig. 4, B and D; cells with decondensed chromatin are denoted by arrows). Furthermore, pretreatment of differentiated HL-60 cells with Cl-amidine inhibited histone citrullination and the formation of NETs (Fig. 4, C and D). The percentages of cells with positive staining of H3 citrullination and/or chromatin decondensation in four independent experiments were counted and are shown in a bar graph (Fig. 4 D). Although a histone H3 citrullination–positive cell may have a round nucleus or a nucleus with decondensed chromatin forming NETs, each nucleus with decondensed chromatin was stained with the histone H3 citrullination antibody. To quantify the amount of chromatin forming NETs, we performed MNase digestion using previously described methods (Fuchs et al., 2007) with slight modifications. Compared with the parental HL-60 cells, we consistently observed an increase in MNase digestion and nucleosomal DNA ladder formation in DMSO-differentiated HL-60 cells after IL-8 and bacteria treatment for 15 h (Fig. 4 E, lanes 4 and 5). Furthermore, MNase digestion was decreased when DMSO-differentiated HL-60 cells were pretreated with the PAD4 inhibitor, Cl-amidine (Fig. 4 E, lanes 5 and 6). Together, the aforementioned immunostaining and MNase analyses indicate that PAD4 activity is required for histone citrullination and NET formation.

Loss of heterochromatin and lobular nuclear morphology in HL-60 granulocytes after calcium ionophore treatment

In electron microscopy analyses, HL-60 granulocytes display a multilobular nuclear structure with distinct heterochromatin underlying the nuclear envelope (Fig. 4, F and G, left). To test whether these characteristic nuclear structures are affected by PAD4 activation, we analyzed nuclear morphology in HL-60 granulocytes by electron microscopy. Without calcium ionophore

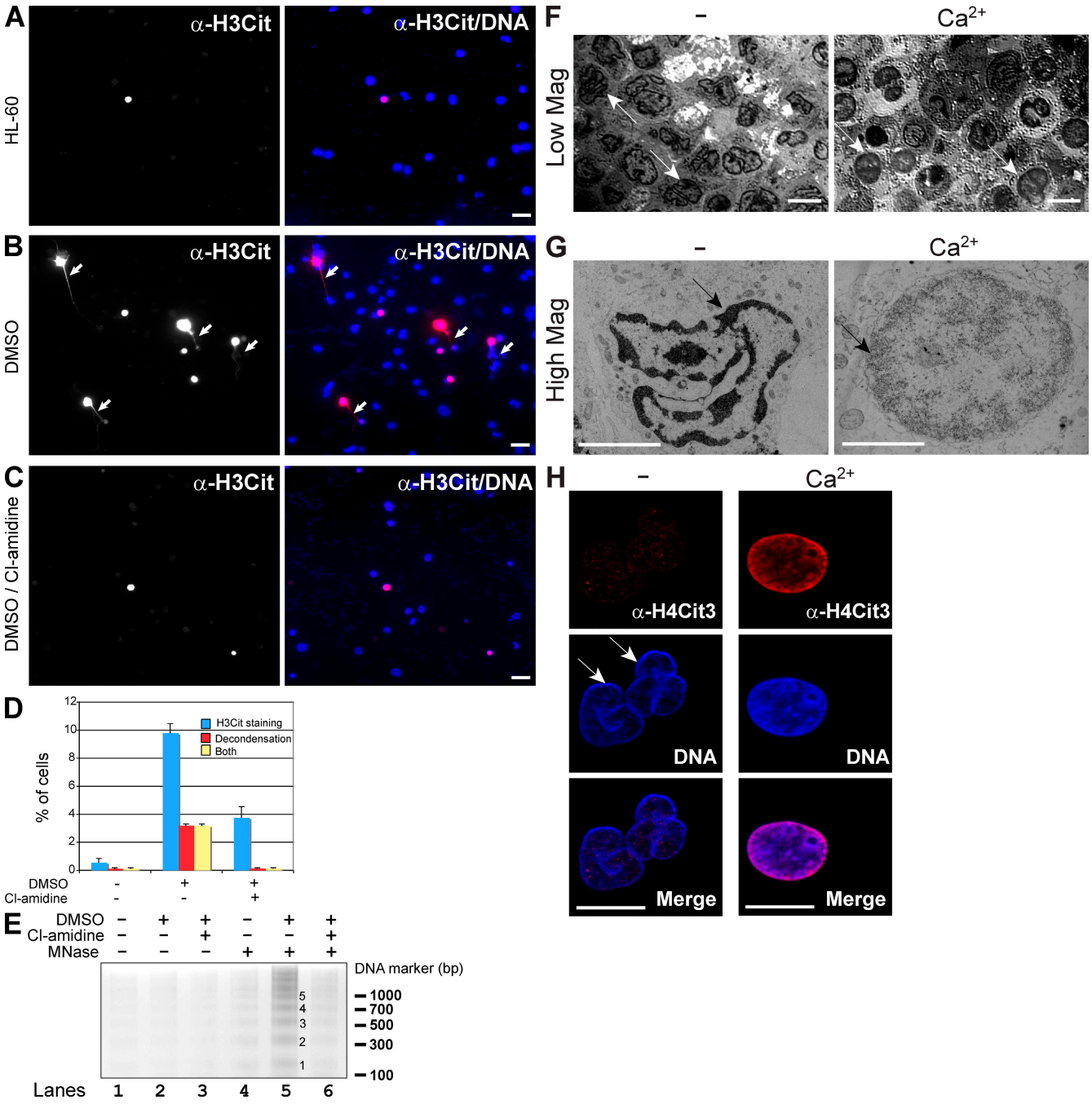

Figure 4. **PAD4 activity is important for NET formation after cytokine and bacteria treatment and for loss of heterochromatin and multilobular nuclear structures.** (A-C) Histone H3 citrullination and DNA staining in undifferentiated HL-60 cells (A), DMSO-differentiated HL-60 cells (B), and DMSO-differentiated HL-60 cells pretreated with Cl-amidine (C) after treatment with IL-8 and bacteria *S. flexneri*. The arrows denote decondensed chromatin stained by the H3Cit antibody. (D) Percentages of cells with positive staining of H3 citrullination and/or chromatin decondensation shown with standard deviations (error bars; $n = 4$; >3,000 cells counted in each experiment). (E) After 15 h of IL-8 and bacteria treatment, NET formation was measured by MNase digestion. Numbers denote mono- and polynucleosomal DNA. (F and G, left) Transmission electron microscopy analyses of HL-60 granulocytes before calcium ionophore treatment. The arrows denote nuclei with distinct heterochromatin (dark regions) underlining the nuclear envelope. (right) Transmission electron microscopy analyses after calcium ionophore treatment. The arrows denote nuclei that lost the distinct heterochromatin structure underlining the nuclear envelope. (H) H4 citrullination and DNA staining before (left column; arrows denote two nuclei) and after calcium ionophore treatment. Notice the loss of both multilobular nuclear structure and rimlike heterochromatin after H4 citrullination. Bars: (A–C) 20 µm; (F and H) 10 µm; (G) 5 µm.

treatment, each HL-60 granulocyte has a rim of electron-dense heterochromatin underlying the nuclear envelope (Fig. 4, F and G, left). In contrast, heterochromatic regions appear more diffuse and electron lucent in ∼35% of cells after calcium ionophore treatment for 15 min (Fig. 4, F and G, right).

To test whether these nuclear structure changes are related to histone citrullination, we performed immunofluorescence analyses. Before calcium treatment, HL-60 granulocyte nuclei showed a clear multilobular structure (Fig. 4 H, left; arrows denote two nuclei). Furthermore, a rimlike structure of heterochromatin

underneath the nuclear envelope and weak H4Cit3 staining were detected (Fig. 4 H). In contrast, after calcium ionophore treatment, nuclei became round and lost the multilobular nuclear structure with a concomitant increase in H4Cit3 staining (Fig. 4 H, right), suggesting that the activation of PAD4 and subsequent histone citrullination caused dramatic changes in HL-60 granulocytes' nuclear structure.

Histone citrullination inhibits nucleosome array folding by linker histone H5

To analyze whether histone citrullination affects the nucleosome compaction, we analyzed the density of the 207 × 12 nucleosome core particle array (Springhetti et al., 2003), which contains 12 nucleosome core particles assembled with core histones H3, H2B, H2A, and H4 on a defined DNA template, treated with GST-PAD4 or the GST-PAD4^{C645S} mutant. The ability of PAD4 to citrullinate nucleosomal histones was confirmed by Western blotting (unpublished data). Consistent with the maintenance of the primary nucleosome structure (Fig. 3 I), there was no difference between the density of the 207 × 12 nucleosome core particle array treated with PAD4 or the PAD4^{C645S} mutant (Fig. 5 A). This result suggests that under current experimental conditions, citrullination of histones by PAD4 did not generate detectable conformation changes in the nucleosomal core particle arrays.

The organization of nucleosome core particles to higher order chromatin structure is mediated by linker histones (Schalch et al., 2005; Brown and Schuck, 2006; Fan and Roberts, 2006; Kan et al., 2007). 207 × 12 nucleosomal core particle arrays sediment at 35 S without linker histone and at 53 S with linker histone added. Next, we used this defined biochemical system to test whether PAD4 treatment affects linker histone–mediated array compaction. After treatment with PAD4 or the PAD4^{C645S} mutant and analytical ultracentrifugation, the peak of the 207 × 12 nucleosomal core particle arrays was recovered, and the linker histone H5 was added to further compact the array. Interestingly, after adding H5, the 207 × 12 nucleosomal core particle array treated by the PAD4^{C645S} mutant and PAD4 formed an ∼50-S and ∼40-S structure, respectively (Fig. 5 B). The 10-S difference in the density of these arrays indicates that citrullination of core histones in the 207 × 12 array by PAD4 decreased the ability of H5 to compact the array.

Because the physiological substrate of PAD4 in cells is chromatin (i.e., nucleosomes associated with linker histones), we further analyzed whether PAD4 can alter the structure of the 207 × 12 array assembled in the presence of H5. The H5-containing 207 × 12 array formed a 53-S structure after treatment with the PAD4^{C645S} mutant (Fig. 5 C), whereas a 45-S structure was formed after treatment with PAD4 (Fig. 5 C). These results show that PAD4 mediates the formation of a less condensed nucleosome array structure.

In summary, our experiments showed that PAD4 and histone hypercitrullination play a unique role in chromatin decondensation in HL-60 granulocytes and peripheral blood neutrophils. Using the HL-60 granulocytes as a model system, we showed that PAD4 activity and histone hypercitrullination are important for the extensive chromatin decondensation during

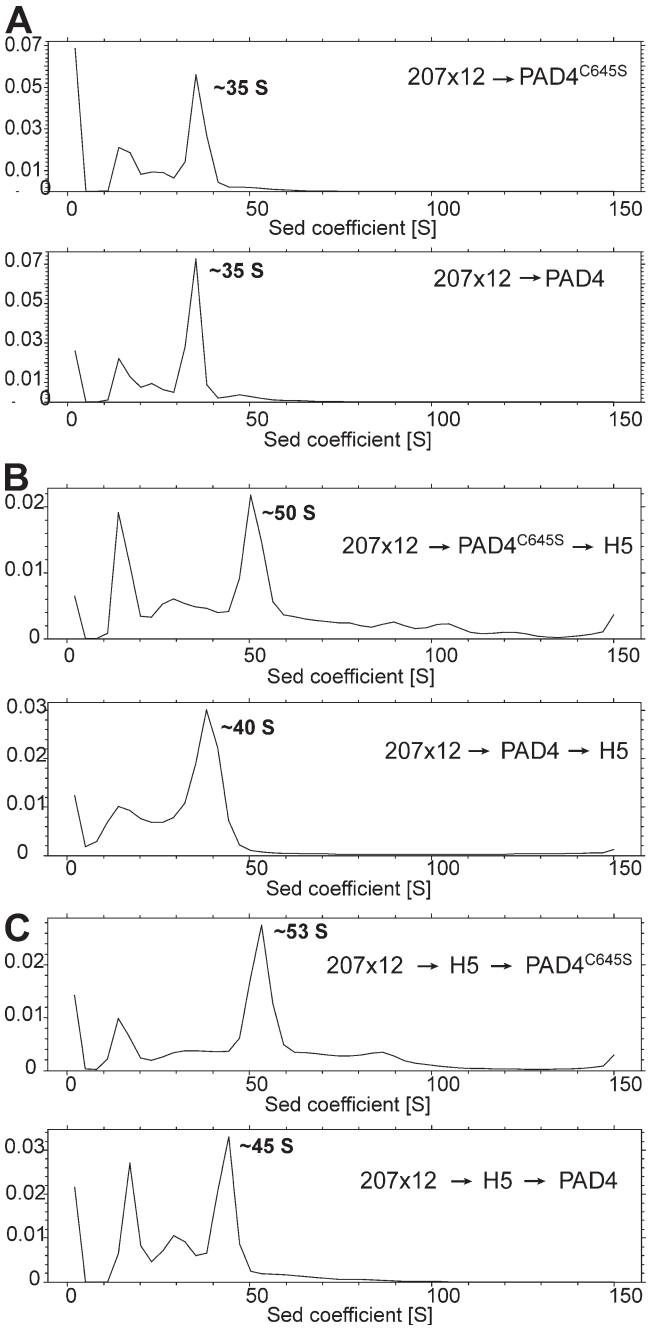

Figure 5. **Histone citrullination inhibits nucleosome array compaction by linker histone H5.** (A) A 35-S structure was detected after treatment of the 207 × 12 array (containing 12 nucleosome core particles in an array) with the GST-PAD4^{C645S} mutant or GST-PAD4. (B) After adding the linker histone H5, the 207 × 12 nucleosome core particle array pretreated with the PAD4^{C645S} mutant was detected as a 50-S structure, whereas the 207 × 12 nucleosome core particle array pretreated with PAD4 was detected as a 40-S structure. (C) The H5-bound 207 × 12 array treated with the PAD4^{C645S} mutant was detected as a 53-S structure, whereas the H5-bound 207 × 12 array treated with PAD4 was detected as a 45-S structure.

NET formation. Because the release of PAD4 into extracellular spaces from neutrophils may generate self-antigens that may induce autoimmune diseases, we envision that the activation of PAD4 and NET formation is an event regulated by multiple signals, including the generation of reactive oxygen species (Fuchs et al., 2007).

Many steps are involved in the formation of a high order chromatin structure in an interphase cell nucleus. The first regulatory step to form a condensed high order chromatin structure is mediated by the association of liker histones to the nucleosome arrays (Trojer and Reinberg, 2007). It is very likely that a decrease in linker histone binding to nucleosomes may help to unfold chromatin during NET formation. We propose that histone citrullination can play a dual role. First, limited citrullination of histones at specific gene promoters regulates gene activity (Cuthbert et al., 2004; Wang et al., 2004; Balint et al., 2005; Li et al., 2008; Yao et al., 2008). Second, global histone hypercitrullination in granulocytes appears to represent one of the underlying mechanisms by which chromatin decondenses during NET formation in granulocytes/neutrophils.

Materials and methods

HL-60 cell differentiation and GST-PAD4 treatments
HL-60 differentiation with DMSO and treatment with calcium ionophore in Locke's solution (10 mM Hepes-HCl, pH 7.3, 150 mM NaCl, 5 mM KCl, 2 mM $CaCl_2$, and 0.1% glucose) were performed essentially as previously described (Wang et al., 2004). To analyze the effects of PAD4 inhibition on histone citrullination and chromatin decondensation, HL-60 granulocytes were pretreated with Cl-amidine at 200-μM concentration for 15 min at 37°C before calcium ionophore treatment. For Triton X-100 and GST-PAD4 treatment, ~10,000 cells in 50 μl of complete medium were added into each well in a 10-well Teflon-coated slide pretreated with poly-L-lysine for 10 min. Cells were settled and attached to the bottom of the slide for 30 min in a 37°C, 5% CO_2 incubator. The medium was removed, and 50 μl PBST (PBS with 0.1% Triton X-100) supplemented with protease inhibitors (1 μg/ml aprotinin and 1 mM PMSF) was added to permeabilize cells for ~2 min. After briefly rinsing the cells twice with PBS, 0.5 μg GST-PAD4 or the GST-PAD4^{C645S} mutant in 50 μl of PAD assay buffer (50 mM Hepes, pH 7.6, 5 mM $CaCl_2$, 5 mM DTT, and 150 mM NaCl, supplemented with 1 μg/ml aprotinin) was added to treat the cells for 2 h at 37°C. After the treatment, cells were fixed with 3.7% paraformaldehyde in PBS containing 1% Triton X-100 and 2% NP-40 and immunostained similarly as other cells. In parallel, cellular proteins were acid extracted to purify histones for Western blotting. Cl-amidine was provided by P.R. Thompson (University of South Carolina, Columbia, SC).

Acid extraction of histones and Western blotting
The acid extraction of histones and Western blotting with H4Cit3 (1:2,000; Millipore), H3Cit (1:3,000; Abcam), and H3 (1:3,000; Abcam) antibodies were performed essentially as previously described (Wang et al., 2004).

Immunostaining and electron microscopy
After fixation of samples with 3.7% paraformaldehyde in PBS supplemented with 1% Triton X-100 and 2% NP-40, cells were washed with PBST three times for 10 min each. After the third wash, cells were blocked first with 2% BSA and 5% normal goat serum in PBST for at least 30 min at RT. Primary antibodies were diluted in PBST supplemented with 2% BSA and 5% normal goat serum as follows: 1:100 H4Arg3Me (Millipore), 1:500 H4Cit3 (Millipore), and 1:100 H4K16Ac (Millipore). Cells were stained with the primary antibodies in a humid chamber overnight at 4°C. After staining, cells were washed with PBST three times for 10 min each. Cells were stained with the appropriate secondary antibodies conjugated with Cy3 at RT for 2 h in the dark. After washing three times for 10 min each, cells were counterstained with 1 μg/ml Hoechst and mounted for imaging with a fluorescence microscope (Axioskop 40; Carl Zeiss, Inc.) using an A-plan 10× NA 0.45 (Carl Zeiss, Inc.) or a Fluar 40× NA 1.30 oil Ph3 objective lens (Carl Zeiss, Inc.). Images were captured using a camera (AxioCam MRM; Carl Zeiss, Inc.) and the Axiovision AC software (Carl Zeiss, Inc.) at RT. Images were further processed and pseudocolored using Photoshop (Adobe) with the appropriate adjustment of levels. Electron microscopy work was performed at the BioImaging Resource Center at the Rockefeller University.

Blood neutrophil isolation and TNF-α treatment
Peripheral neutrophils were used according to the Institutional Review Board–approved protocols of the Weill Medical School of Cornell University. Neutrophils were isolated to >95% purity using Polymorphprep (Axis-Shield PoC AS) and treated with TNF-α as previously described (Han et al., 2005).

MNase digestion of HL-60 cells after permeabilization with Triton X-100
After cells were permeabilized with PBST (0.1% Triton X-100) and treated with GST-PAD4 or the GST-PAD4^{C645S} mutant, cells were collected by spinning at 2,000 rpm for 10 min at 4°C. The cell pellet was resuspended in 250 μl of buffer N2 (10 mM Pipes, pH 6.5, 0.5 mM sodium metabisulfate, 0.5 mM benzamidine-HCl, and 5 mM $MgCl_2$ freshly supplemented with 0.5 mM DTT and 0.1 mM PMSF). The samples were kept on ice, and 0.5 U RNase A and $CaCl_2$ was added to 5 mM. MNase (the amount of MNase was optimized for each batch; Sigma-Aldrich) was added to a 50-μl reaction. Reactions were performed at 37°C and stopped at 0, 5, 10, and 15 min by increasing the EDTA concentration to 10 mM. Then, 75 μl H_2O, 30 μl of 10% SDS, 25 μl of 4 M NaCl, and 200 μl phenol-chloroform were added to the digested samples in a sequential order and mixed by vortex. Samples were centrifuged at 13,000 rpm for 10 min. 1/3 vol of 7.5 M NH_4Ac, pH 7.6, and 1 vol of isopropanol were added in a sequential order. Samples were left at RT for 10 min to precipitate DNA and centrifuged at 13,000 rpm for 10 min. DNA was washed with cold 70% ethanol three times to remove salt, air dried, resuspended in 10 μl H_2O, and analyzed in 1.5% DNA agarose gel.

IL-8 and *S. flexneri* treatment of HL-60 cells and MNase digestion to analyze DNA release during NET formation
HL-60 cells were treated with 1.25% DMSO for 3 d for differentiation. For Cl-amidine treatment, differentiated HL-60 cells were preincubated with 200 μM Cl-amidine for 1 h to inhibit PAD4 activity. Then, 3×10^5 cells from each group (HL-60 cells, differentiated HL-60 cells, and differentiated HL-60 cells pretreated with Cl-amidine) were resuspended in Locke's solution (10 mM Hepes-HCl, pH 7.3, 150 mM NaCl, 5 mM KCl, 2 mM $CaCl_2$, and 0.1% glucose) supplemented with 0.1% FBS and spun down to coverslips by centrifugation at 700 *g* for 10 min. Cells were incubated with 100 ng/ml IL-8 for 30 min. 3×10^7 exponential-phase *S. flexneri* were added to cells (MOI =100) and spun at 200 *g* for 10 min. Cells were incubated for 3 h in a 5% CO_2, 37°C incubator before immunostaining analyses or for 15 h to increase NET formation before MNase treatment to measure DNA release. For MNase treatment, after incubation with *S. flexneri* for 15 h, DTT and Ca^{2+} were added to the sample to a final concentration of 1 mM and 5 mM, respectively. Samples were incubated with 0.5 U MNase for 3 min at RT, and the reaction was stopped by adding 20 mM EDTA. Samples were centrifuged at 200 *g* for 5 min, and supernatant was collected for DNA extraction. Released DNA was extracted using phenol-chloroform, ethanol precipitated, and analyzed in 1.2% agarose gels.

Nucleosome array reconstitution, PAD4 reaction, and analytical ultracentrifugation
Nucleosome positioning templates containing 12 clone 601 repeats uniformly positioned every 207 bp (207 × 12) were constructed and reconstituted with core histones isolated from chicken erythrocytes as previously described (Nikitina et al., 2007). Competitor DNA was obtained from the pUC19 vector and added to the reconstitution mixture at a template DNA to competitor DNA ratio of 2:1. The reconstituted nucleosome core arrays were purified on a sucrose gradient. Purified fractions were collected, dialyzed for 48 h against 10 mM Hepes, pH 7.5, 0.1 mM EDTA, and 5 mM NaCl, and concentrated to A_{260} = ~2.0. For linker arrays, linker histone H5 was isolated from chicken erythrocytes and reconstituted with the core arrays at a ratio of one molecule of H5 per nucleosome.

PAD4 was incubated with either core arrays or linker arrays. Reaction mixtures contained 0.1 μg PAD4 per 1 μg histone with 20 mM Tris, pH 7.5, 2 mM $CaCl_2$, and 2 mM DDT and were incubated for 1 h at 37°C. Control reactions were performed the same way but using the inactive mutant form, PAD4^{C645S}, with either the core or linker arrays. After incubation, EDTA was added to a concentration of 2 mM to stop the reaction. The reaction mixtures were analyzed on 18% SDS-PAGE and by analytical ultracentrifugation. After analytical ultracentrifugation of the PAD4 core arrays, linker histone H5 was added to the centrifuged sample at a ratio of one molecule of H5 per nucleosome and incubated for 1 h at 20°C before repeating the analytical ultracentrifugation.

Sedimentation velocity experiments were conducted to examine nucleosome array compaction using an ultracentrifuge (Optima XL-A; Beckman Coulter). Samples were centrifuged in 150 mM NaCl at 20,000 rpm and 20°C for ~3 h. Data analysis was performed using the continuous c(s) distribution model (Brown and Schuck, 2006) with SEDFIT software (http://www.analyticalultracentrifugation.com).

Online supplemental material

Fig. S1 shows the increase of histone citrullination and chromatin decondensation in HL-60 granulocytes after calcium ionophore treatment and the increase of PAD4 expression in HL-60 cells after DMSO differentiation. Online supplemental material is available at http://www.jcb.org/cgi/content/full/jcb.200806072/DC1.

We thank colleagues in the Allis, Coonrod, and Wang laboratories for discussions and suggestions during the course of this study. We thank the Bio-Imaging Center at the Rockefeller University for electron microscopy support. We thank Dr. Paul R. Thompson and Dr. Na Xiong (Pennsylvania State University) for critical reading of the manuscript.

This research is supported in part by a Pennsylvania State University start-up fund to Y. Wang, an Era of Hope Scholar Award (grant W871XWH-07-1-0372) to S.A. Coonrod, and a National Science Foundation grant (MCB-0615536) to S.A. Grigoryev.

Submitted: 12 June 2008
Accepted: 18 December 2008

References

Balint, B.L., A. Szanto, A. Madi, U.M. Bauer, P. Gabor, S. Benko, L.G. Puskas, P.J. Davies, and L. Nagy. 2005. Arginine methylation provides epigenetic transcription memory for retinoid-induced differentiation in myeloid cells. *Mol. Cell. Biol.* 25:5648–5663.

Beiter, K., F. Wartha, B. Albiger, S. Normark, A. Zychlinsky, and B. Henriques-Normark. 2006. An endonuclease allows *Streptococcus pneumoniae* to escape from neutrophil extracellular traps. *Curr. Biol.* 16:401–407.

Brinkmann, V., U. Reichard, C. Goosmann, B. Fauler, Y. Uhlemann, D.S. Weiss, Y. Weinrauch, and A. Zychlinsky. 2004. Neutrophil extracellular traps kill bacteria. *Science*. 303:1532–1535.

Brown, P.H., and P. Schuck. 2006. Macromolecular size-and-shape distributions by sedimentation velocity analytical ultracentrifugation. *Biophys. J.* 90:4651–4661.

Buchanan, J.T., A.J. Simpson, R.K. Aziz, G.Y. Liu, S.A. Kristian, M. Kotb, J. Feramisco, and V. Nizet. 2006. DNase expression allows the pathogen group A *Streptococcus* to escape killing in neutrophil extracellular traps. *Curr. Biol.* 16:396–400.

Cuthbert, G.L., S. Daujat, A.W. Snowden, H. Erdjument-Bromage, T. Hagiwara, M. Yamada, R. Schneider, P.D. Gregory, P. Tempst, A.J. Bannister, and T. Kouzarides. 2004. Histone deimination antagonizes arginine methylation. *Cell*. 118:545–553.

Fan, L., and V.A. Roberts. 2006. Complex of linker histone H5 with the nucleosome and its implications for chromatin packing. *Proc. Natl. Acad. Sci. USA*. 103:8384–8389.

Fuchs, T.A., U. Abed, C. Goosmann, R. Hurwitz, I. Schulze, V. Wahn, Y. Weinrauch, V. Brinkmann, and A. Zychlinsky. 2007. Novel cell death program leads to neutrophil extracellular traps. *J. Cell Biol.* 176:231–241.

Hagiwara, T., K. Nakashima, H. Hirano, T. Senshu, and M. Yamada. 2002. Deimination of arginine residues in nucleophosmin/B23 and histones in HL-60 granulocytes. *Biochem. Biophys. Res. Commun.* 290:979–983.

Han, H., A. Stessin, J. Roberts, K. Hess, N. Gautam, M. Kamenetsky, O. Lou, E. Hyde, N. Nathan, W.A. Muller, et al. 2005. Calcium-sensing soluble adenylyl cyclase mediates TNF signal transduction in human neutrophils. *J. Exp. Med.* 202:353–361.

Jenuwein, T., and C.D. Allis. 2001. Translating the histone code. *Science*. 293:1074–1080.

Kan, P.Y., X. Lu, J.C. Hansen, and J.J. Hayes. 2007. The H3 tail domain participates in multiple interactions during folding and self-association of nucleosome arrays. *Mol. Cell. Biol.* 27:2084–2091.

Kornberg, R.D., and Y. Lorch. 1999. Twenty-five years of the nucleosome, fundamental particle of the eukaryote chromosome. *Cell*. 98:285–294.

Kouzarides, T. 2007. Chromatin modifications and their function. *Cell*. 128:693–705.

Li, B., M. Carey, and J.L. Workman. 2007. The role of chromatin during transcription. *Cell*. 128:707–719.

Li, P., H. Yao, Z. Zhang, M. Li, Y. Luo, P.R. Thompson, D.S. Gilmour, and Y. Wang. 2008. Regulation of p53 target gene expression by peptidylarginine deiminase 4. *Mol. Cell. Biol.* 28:4745–4758.

Luo, Y., K. Arita, M. Bhatia, B. Knuckley, Y.H. Lee, M.R. Stallcup, M. Sato, and P.R. Thompson. 2006. Inhibitors and inactivators of protein arginine deiminase 4: functional and structural characterization. *Biochemistry*. 45:11727–11736.

Nakashima, K., T. Hagiwara, A. Ishigami, S. Nagata, H. Asaga, M. Kuramoto, T. Senshu, and M. Yamada. 1999. Molecular characterization of peptidylarginine deiminase in HL-60 cells induced by retinoic acid and 1alpha,25-dihydroxyvitamin D(3). *J. Biol. Chem.* 274:27786–27792.

Nakashima, K., T. Hagiwara, and M. Yamada. 2002. Nuclear localization of peptidylarginine deiminase V and histone deimination in granulocytes. *J. Biol. Chem.* 277:49562–49568.

Neeli, I., S.N. Khan, and M. Radic. 2008. Histone deimination as a response to inflammatory stimuli in neutrophils. *J. Immunol.* 180:1895–1902.

Nikitina, T., R.P. Ghosh, R.A. Horowitz-Scherer, J.C. Hansen, S.A. Grigoryev, and C.L. Woodcock. 2007. MeCP2-chromatin interactions include the formation of chromatosome-like structures and are altered in mutations causing Rett syndrome. *J. Biol. Chem.* 282:28237–28245.

Richmond, T.J., and C.A. Davey. 2003. The structure of DNA in the nucleosome core. *Nature*. 423:145–150.

Robinson, P.J., W. An, A. Routh, F. Martino, L. Chapman, R.G. Roeder, and D. Rhodes. 2008. 30 nm chromatin fibre decompaction requires both H4-K16 acetylation and linker histone eviction. *J. Mol. Biol.* 381:816–825.

Schalch, T., S. Duda, D.F. Sargent, and T.J. Richmond. 2005. X-ray structure of a tetranucleosome and its implications for the chromatin fibre. *Nature*. 436:138–141.

Shilatifard, A. 2006. Chromatin modifications by methylation and ubiquitination: implications in the regulation of gene expression. *Annu. Rev. Biochem.* 75:243–269.

Springhetti, E.M., N.E. Istomina, J.C. Whisstock, T. Nikitina, C.L. Woodcock, and S.A. Grigoryev. 2003. Role of the M-loop and reactive center loop domains in the folding and bridging of nucleosome arrays by MENT. *J. Biol. Chem.* 278:43384–43393.

Strahl, B.D., and C.D. Allis. 2000. The language of covalent histone modifications. *Nature*. 403:41–45.

Su, A.I., T. Wiltshire, S. Batalov, H. Lapp, K.A. Ching, D. Block, J. Zhang, R. Soden, M. Hayakawa, G. Kreiman, et al. 2004. A gene atlas of the mouse and human protein-encoding transcriptomes. *Proc. Natl. Acad. Sci. USA*. 101:6062–6067.

Trojer, P., and D. Reinberg. 2007. Facultative heterochromatin: is there a distinctive molecular signature? *Mol. Cell*. 28:1–13.

Turner, B.M. 2000. Histone acetylation and an epigenetic code. *Bioessays*. 22:836–845.

Vossenaar, E.R., A.J. Zendman, W.J. van Venrooij, and G.J. Pruijn. 2003. PAD, a growing family of citrullinating enzymes: genes, features and involvement in disease. *Bioessays*. 25:1106–1118.

Wang, Y., J. Wysocka, J. Sayegh, Y.H. Lee, J.R. Perlin, L. Leonelli, L.S. Sonbuchner, C.H. McDonald, R.G. Cook, Y. Dou, et al. 2004. Human PAD4 regulates histone arginine methylation levels via demethylimination. *Science*. 306:279–283.

Yao, H., P. Li, B.J. Venters, S. Zheng, P.R. Thompson, B.F. Pugh, and Y. Wang. 2008. Histone Arg modifications and p53 regulate the expression of OKL38, a mediator of apoptosis. *J. Biol. Chem.* 283:20060–20068.